Oxygen-associated holelike centers in calcium chlorapatite*

A. Roufosse, M. Stapelbroek, R. H. Bartram, and O. R. Gilliam
Department of Physics and Institute of Materials Science, University of Connecticut, Storrs, Connecticut 06268
(Received 28 August 1973)

Single crystals of calcium chlorapatite $Ca_5(PO_4)_3Cl$ grown from $CaCl_2$ flux in air show two holelike spin-1/2 defects by ESR after x irradiation at 300 K. Both defects are axially symmetric about the pseudohexagonal c axis of the monoclinic structure. One defect exhibits partially resolved hyperfine interaction with the nuclei of three inequivalent chlorine ions. The hole is shared primarily by an O^{2-} impurity ion (substitutional for Cl^-) and a nearest-neighbor Cl^- ion (site 1); it is shared weakly with the other nearest-neighbor Cl^- ion (site 2); and a next-nearest neighbor Cl^-ion (site 3). The oxygen and chlorine ions lie in successive sites along the screw axis. Spin-Hamiltonian parameters obtained by fitting computer-simulated spectra to observed spectra are $g_{\parallel} = 2.0031$, $g_{\perp} = 2.0255$, for Cl^{35} in units of gauss $|A_{\parallel}|^{(1)} = 30.3$, $|A_{\perp}|^{(1)} = 13.5$, $|A_{\parallel}|^{(2)} = 1.55$, $|A_{\perp}|^{(2)} = 0.80$, $|A_{\parallel}|^{(3)} = 0.94$, and $|A_{\perp}|^{(3)} = 0.40$. An approximate wave function for this hole was constructed from a linear combination of valence orbitals of adjacent oxygen and chlorine ions using one adjustable parameter. Hyperfine interactions calculated with this wave function agree closely with the experimental values. The second defect shows a single line with $g_{\parallel} = 2.0032$ and $g_{\perp} = 2.0386$; an O^- ion adjacent to a Cl^- vacancy is suggested as a model.

I. INTRODUCTION

Natural and synthetic calcium apatites $Ca_5(PO_4)_3X$, where X represents Cl, F, or OH, are of interest to a diverse group of researchers. Hydroxyapatite is of biological significance since it is the major inorganic constituent of bone and dental tissues. Apatites found in geological ores are important for agriculture as a source of phosphate. Technological applications of synthetic apatites include the use of mixed chlor- and fluorapatites doped with manganese and antimony for efficient phosphors in fluorescent lights, the growth of large single crystals of neodynium-doped fluorapatite for lasers, and the employment of apatitic materials for catalysis. Numerous references to researches on apatites are given in review articles by Elliott,[1] Montel,[2] and Richelle and Onkelinx.[3] Investigations are more complete in fluorapatite for which good quality single crystals are more easily obtained. Also this apatite has a hexagonal crystal structure[4,5] which is of higher symmetry than high-purity stoichiometric chlorapatite[5,6] and hydroxyapatite,[7-9] both of which have monoclinic structures.

Electron-spin resonance (ESR) has been applied by several investigators to study the defect structure of apatites. The first results were obtained on synthetic single crystals of hexagonal fluorapatite $Ca_5(PO_4)_3F$ by Segall *et al.*[10] These authors reported on a paramagnetic holelike center produced by x irradiation, which they attributed to a hole localized on an oxygen impurity ion substitutional for a fluorine ion. Subsequently, a large number of papers were published describing defects in fluorapatite. These include the optical-absorption studies of Swank,[11] ESR and optical studies by Piper *et al.*,[12] Prener *et al.*,[13] and Warren.[14,15]

Similar studies on chlorapatite untwinned synthetic single crystals, $Ca_5(PO_4)_3Cl$, have not been reported until recently. Piper and Prener have reported on the Mn^{2+} ion in chlorapatite.[16] Knotterus *et al.*[17] have reported on optical and ESR investigations of color centers in x-irradiated chlorapatite. In the latter paper the authors interpret a complex hyperfine interaction associated with one of the holelike centers (designated as defect I) as resulting from an electron deficiency interacting with nuclei in two inequivalent chlorine-ion positions. We are in disagreement with their interpretation of this defect. Our computer-simulated fit of the spectrum shows that the hyperfine interaction is with nuclei in three inequivalent chlorine-ion positions. The model that we have selected for this defect, in contrast to theirs, does not have a vacancy adjacent to the impurity oxygen ion. Also, we conclude that the unpaired spin is shared by the oxygen ion and an adjacent chlorine ion rather than being localized on that chlorine ion as they have reported. For a second holelike defect which contributes only a single resonance line to the ESR spectrum (defect II), Knotterus *et al.*[17] have suggested as a tentative model a hole associated with two oxygen ions sandwiched between two chlorine-ion vacancies. We propose a less complex model consisting of an O^- ion near a Cl^--ion vacancy. For this defect the hole is more localized on the oxygen than for the other holelike defect; thus hyperfine interactions with nearby chlorine nuclei are small and only a single line is observed. The present paper is concerned primarily with interpretation of the ESR results for defect I.

II. CRYSTAL STRUCTURE

The basic apatitic structure is described by the hexagonal space group $P6_3/m$.[4] This is the space

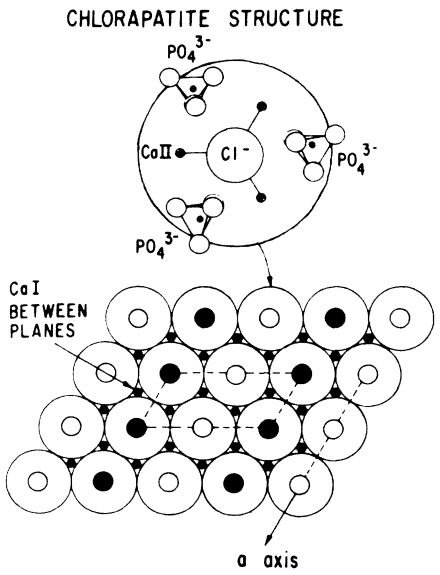

FIG. 1. Monoclinic lattice structure of chlorapatite $Ca_5(PO_4)_3Cl$ projected onto the basal plane. An expanded view at the top of the drawing shows the ion arrangement inside each large circle. The parallelogram depicts the base of a unit cell. (Reproduced from Ref. 16 with permission.)

group most often found in naturally occurring apatites and in synthetic fluorapatite and chlorapatite grown from the melt at a temperature of about 1650 °C. Such high-temperature growth gives a large number of vacancies, especially for chlorapatite which gives off $CaCl_2$ at high temperatures.[5,18] An important deviation from hexagonal symmetry has been found for synthetic chlorapatite grown from solution in $CaCl_2$ flux in the temperature range 1200–1050 °C.[5] Such crystals are more stoichiometric (3–5% chlorine deficient) than those grown at the melting point and satisfy the monoclinic space group $P2_1/b$.[5,6] This monoclinic form, which is often called pseudohexagonal, undergoes a phase transition to hexagonal symmetry at approximately 205 °C. When cooled through the transition temperature, the monoclinic structure is assumed by different parts of the crystal concurrently giving rise to twinning. From flux-growth runs it has been possible, however, to select untwinned specimens having dimensions in the mm range.

Figure 1 represents the monoclinic chlorapatite structure for a portion of the unit cell projected onto a plane perpendicular to the pseudohexagonal c axis. The unit cell is shown by the dotted quadrangle where the smaller and larger cell dimensions are along the a and b axes, respectively. Important to this investigation are the locations of chlorine ions, which lie along the screw axis for the monoclinic crystal. Figure 2 depicts a screw-axis environment. For a given plane containing the a and screw axes the chlorine ions reside in the lower of two oxygen-ion triangles which are between neighboring calcium-ion triangles. For the adjacent parallel plane (displaced along the b axis) the chlorine ions reside in the upper of the neighboring oxygen triangles. For fluorapatite the F^- ion occupies the center of the calcium triangle; this is precluded for Cl^- in chlorapatite because of its larger ionic radius. The unit-cell dimensions for monoclinic chlorapatite are $a = 9.628$ Å, $b = 12.256$ Å, and $c = 6.764$ Å and the distance between two chlorine ions on the c axis is 3.382 Å.[6]

III. EXPERIMENTAL

The chlorapatite crystals employed for this study, which were furnished by Kostiner of this laboratory, were monoclinic crystals grown from a $CaCl_2$ flux. In this method nearly stoichiometric crystals with hexagonal shape were obtained by slowly cooling a saturated solution of chlorapatite in $CaCl_2$ from 1200 to 1050 °C. Some recycling was used to enhance the size of the crystals. Crystals were grown in both air and HCl atmospheres. The former atmosphere is believed to yield the incorporation of a small percentage of oxygen impurity ions substitutional for Cl^- ions and the introduction of a corresponding number of charge-compensating Cl^--ion vacancies. The HCl atmosphere is believed to yield purer more-stoichiometric crystals. Most of the chlorapatite crystals[18] showed twinning; however, untwinned crys-

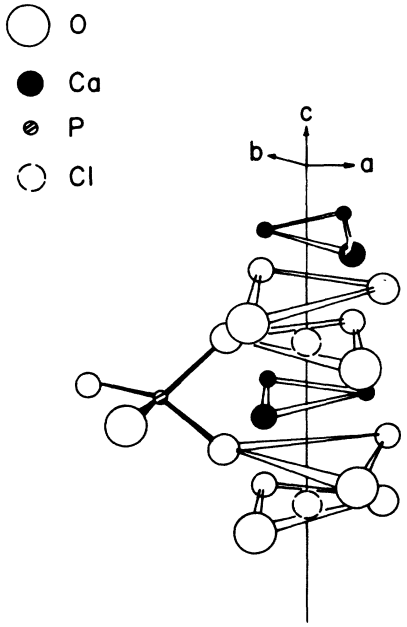

FIG. 2. Schematic representation of the environment of a Cl-ion column in chlorapatite (perspective view).

tals as large as 5×2×2 mm were selected for these experiments.

ESR observations were made at 300 K with Varian E-3 and E-12 *X*-band spectrometers using 100-kHz magnetic-field modulation. Precise measurements of magnetic field were made by proton resonance; the microwave frequency was measured by electronic counter. A weak ESR absorption from the holelike center exhibiting hyperfine structure was observed in the oxygen-containing crystals prior to irradiation; however, the single-line holelike defect was not detected. Strong absorptions from both defects were obtained at 300 K after 30-min irradiation using an unfiltered x-ray beam (Mo target, 40 kV, 15 mA). The irradiation also caused the crystal to change from colorless to brown. The holelike defects described here are not associated with this coloration. The coloration does, however, appear to be associated with defects which were observed by ESR at liquid-nitrogen temperature immediately after the room-temperature irradiation. These defects and the coloration can be eliminated by exposure to room light at 300 K for about one day. The holelike defects which are the subject of this paper remain at about the same intensity as before this treatment.

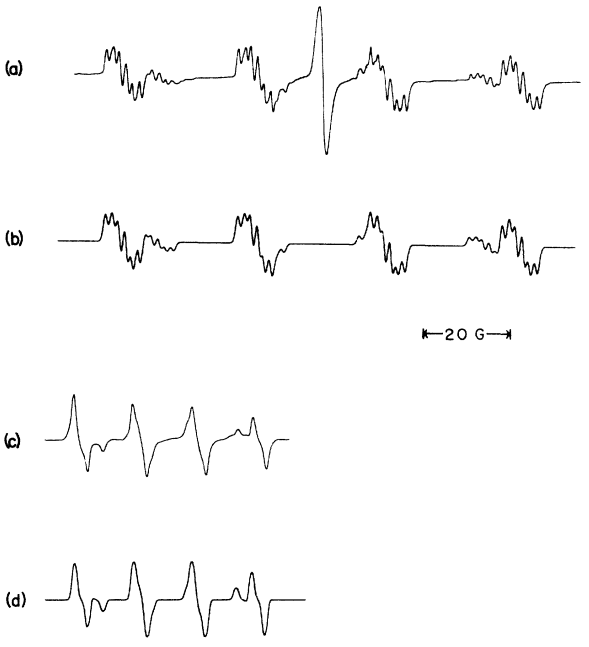

FIG. 3. (a) Observed ESR spectrum of two holelike defects in x-irradiated chlorapatite flux grown in air, one defect yielding a single line and the other a complex hyperfine interaction with nuclei in three inequivalent chlorine ion sites ($\vec{H} \| \vec{c}$); (b) computer-simulated ESR spectrum for hole with hyperfine structure ($\vec{H} \| \vec{c}$); (c) observed ESR spectrum for the same defects with $\vec{H} \perp \vec{c}$; and (d) computer-simulated ESR spectrum for hole with hyperfine splitting ($\vec{H} \perp \vec{c}$). All spectra observed at 300 K and 9.55 GHz.

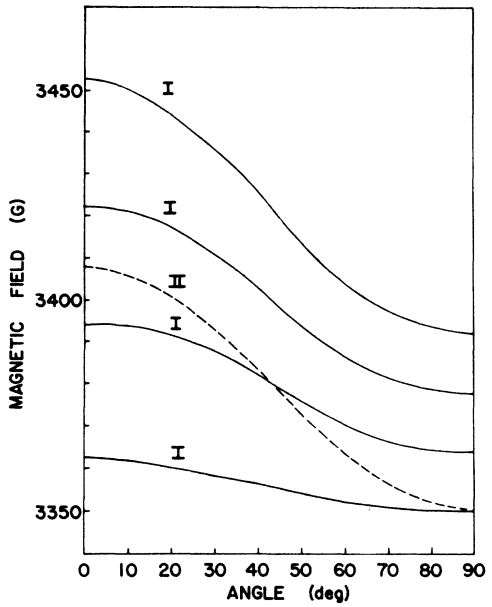

FIG. 4. Angular variations of ESR absorptions for holelike defects I and II in chlorapatite calculated from experimental spin-Hamiltonian parameters. Defect II gave a single resonance line. For defect I only the four-line hyperfine interaction with a Cl^{35} isotope in site 1 is shown. All spectra observed at 300 K and 9.55 GHz.

IV. ESR RESULTS

The two holelike centers detected at 300 K by ESR after a room-temperature x irradiation were in chlorapatite crystals that were flux grown in air. They were not detected in chlorapatite which was flux grown in an HCl atmosphere. Neither were they observed in chlorapatite which was grown hydrothermally in 1*N* hydrochloric acid.[19] ESR spectra are shown in Figs. 3(a) and 3(c) for orientations respectively parallel and perpendicular to the pseudohexagonal *c* axis; this axis is found to be an axis of symmetry for both defects. These centers correspond to spin-$\frac{1}{2}$ holelike defects. One of the centers exhibits a hyperfine interaction with the nuclei in three inequivalent chlorine sites; however, the hyperfine tensor for one site is much larger than for the other two; the second center exhibits a single line. The following conventions will be used to describe the defects: The symbol (I) will signify the defect whose ESR spectrum shows a complex hyperfine splitting and (II) will signify the defect having the single resonance line. The chlorine-ion positions related to the defect will be designated 1, 2, and 3 in the order of decreasing hyperfine interaction. The spectrum for (I) is complex because each of the three chlorine

sites can be occupied by either Cl^{35} (75.53% abundant) or Cl^{37} (24.47%) isotopes, which both have nuclear spins of $\frac{3}{2}$, but nuclear magnetic moments of $0.82088\mu_N$ and $0.68328\mu_N$, respectively.[20] The angular variation for the ESR spectra of defects I and II are shown in Fig. 4; for defect I only the resonances corresponding to hyperfine interaction with a Cl^{35} nucleus in site 1 are shown.

The ESR spectrum for $\vec{H} \perp \vec{c}$, [Fig. 3(c)] shows four major lines with approximately equal spacing and equal intensity characteristic of hyperfine interaction with a single spin-$\frac{3}{2}$ nucleus. Closer examination indicates a second set of four equally spaced lines having intensity about one-third that of the larger set and constant splittings about 0.8 as large. This set is only partially resolved from the larger set. These sets of lines are attributed to hyperfine interaction of the defect with a nearest-neighbor chlorine nucleus (site 1), the two sets resulting from the isotope effect. For $\vec{H} \parallel \vec{c}$ [Fig. 3(a)], additional splittings or superhyperfine structures are observed. There are too many lines for interaction with just one additional chlorine nucleus. Also each component of the larger four-line set has an intensity distribution which looks somewhat like that expected from a superhyperfine interaction with two chlorine nuclei (sites 2 and 3). As an example, if the chlorine ion positions 2 and 3 were equivalent and were each occupied by a Cl^{35} nucleus, then a seven-line superhyperfine pattern would result with an intensity ratio of 1 : 2 : 3 : 4 : 3 : 2 : 1. Allowance for Cl^{35}-Cl^{37} and Cl^{37}-Cl^{37} combinations, however, would account for a poor resolution and a modification of this intensity ratio. Furthermore, an inequivalency of ion positions 2 and 3 would be expected to cause even greater reduction in resolution and change in intensity characteristics. To test whether the spectrum could be explained on the basis of hyperfine and superhyperfine interactions, computer-simulated spectra were generated with various trial values of interaction constants. The computer program was devised to add derivatives of Gaussian absorption lines; provision was made for isotope effects, for adjustment of the hyperfine interaction parameters with each of the inequivalent chlorines, and for adjustment of Gaussian linewidth. The best computer-generated spectra are shown in Figs. 3(b) and 3(d); they are seen to compare favorably with the experimentally observed spectra. For the computer-simulated spectra in Figs. 3(b) and 3(d) the selected Gaussian linewidths between inflection points were 1.05 and 0.85 G, respectively. Lorentzian line shapes were also tried, but they did not yield as good a fit.

Defect I can be represented by the spin Hamiltonian

$$\mathcal{H} = \mu_B[g_{\parallel} S_z H_z + g_{\perp}(S_x H_x + S_y H_y)] + \sum_i [A_{\parallel}^{(i)} S_z I_z + A_{\perp}^{(i)}(S_x I_x + S_y I_y) - g_N \mu_N \vec{H} \cdot \vec{I}_i] , \quad (1)$$

where i differs for different sites and for different chlorine isotopes. Defect II can be represented by the same Hamiltonian with the elimination of the hyperfine terms. The measured parameters for defects I and II are summarized in Table I. These measurements were made in untwinned crystals. Both defects appeared axial within experimental error. For twinned crystals that were examined, the superhyperfine structure shown in Fig. 3(a) appeared somewhat more complex; however, the reason for the added complexity was not investigated.

The spin-Hamiltonian parameters for defect I suggested a model consisting of a hole shared primarily between an O^{2-} impurity (substitutional for a Cl^- ion) and one of the two adjacent chlorine ions. It is also shared with the other Cl^- ion adjacent to the O^{2-} ion and with a next-nearest-neighbor Cl^- ion. This model is represented in Fig. 5 in which the positively charged hole is represented by the symbol h and the inequivalent Cl^--ion positions described previously are labeled 1, 2, and 3. Defect II, represented in Fig. 6, is believed to be related to defect I since it is also associated with an oxygen impurity ion; however, the chlorine ion nearest to the oxygen is assumed missing which causes the hole h to localize on the O^{2-} ion, converting it to an O^- ion. Further justification for these models is deferred to Sec. VI.

TABLE I. Spin-Hamiltonian parameters for defects I and II in x-irradiated chlorapatite for measurements at 300 K and 9.55 GHz. Magnitudes of the A tensor components are given for the Cl^{35} isotope in gauss; those for the Cl^{37} isotope are obtained from these by multiplying by the ratio of the magnetic moments.

	Defect I	Defect II
$g_{\parallel}$	2.0031 ± 0.0002	2.0032 ± 0.0002
$g_{\perp}$	2.0255 ± 0.0002	2.0386 ± 0.0002
$A_{\parallel}^{(1)}$	30.3 ± 0.05	No observed hyperfine structure
$A_{\perp}^{(1)}$	13.5 ± 0.10	
$A_{\parallel}^{(2)}$	1.55 ± 0.05	
$A_{\perp}^{(2)}$	0.80 ± 0.10	
$A_{\parallel}^{(3)}$	0.94 ± 0.05	
$A_{\perp}^{(3)}$	0.40 ± 0.10	

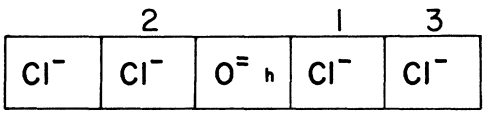

FIG. 5. Model for holelike defect I in chlorapatite representing the negative-ion column along the c axis. Hyperfine interactions are observed with Cl^{35} and Cl^{37} nuclear magnetic moments in three inequivalent chlorine sites. The site numbering has been chosen to increase with decreasing hyperfine interaction. The symbol h is used to represent the hole since it is shared by the O^{2-} ion and an adjacent Cl^- ion.

V. THEORETICAL CALCULATIONS

A. Nature of the wave function

The purpose of the following calculation is to construct a wave function for the trapped hole (defect I) observed by ESR in x-irradiated chlorapatite crystals. In this calculation we are testing the model for the defect shown in Fig. 5 by constructing a wave function containing a single adjustable parameter for the hole. The predictions from this wave function are compared with experimental values for the hyperfine and superhyperfine interaction constants with the chlorines 1, 2, and 3.

An approximate wave function for the defect is constructed from valence orbitals of O^- and $Cl^0 1$. The requirement is that the wave function for the trapped hole be orthogonal to the ion-core orbitals of the neighboring ions. The mutual overlap of ion-core orbitals for ions centered on different lattice sites is very small and will be neglected. However, the overlaps between the hole wave function and the core orbitals of the neighboring ions are larger. They are accounted for by rendering the wave function of the hole orthogonal to the ion-core orbitals by the Schmidt orthogonalization process. If ϕ_h is the wave function chosen for the hole and ϕ_i the core orbitals of the neighboring ions, then the wave function obeying the requirement is

$$\psi_h = N\left(\phi_h - \sum_i \langle \phi_i | \phi_h \rangle \phi_i\right) , \tag{2}$$

where N is a normalizing factor.

B. Magnetic hyperfine interaction spin Hamiltonian

The hyperfine interactions observed by ESR are due to the interaction of the spin magnetic moment of the holelike defect with nuclear magnetic moments of nuclei in three different chlorine ion sites. For axial symmetry where z is the symmetry axis, the hyperfine part of the spin Hamiltonian can be written

$$\mathcal{H}_N = A_{\parallel} S_z I_z + A_{\perp}(S_x I_x + S_y I_y) ,$$

where

$$A_{\parallel} = a + 2b, \quad A_{\perp} = a - b . \tag{3}$$

The value of the isotropic hyperfine constant a can be shown to be proportional to the electron density at the nucleus:

$$a = \tfrac{8}{3}\pi g_e \mu_B g_N \mu_N |\psi_h(0)|^2 . \tag{4}$$

The value of the anisotropic hyperfine constant b, due to dipole-dipole interaction, is

$$b = \tfrac{2}{5} g_e \mu_B g_N \mu_N (1/r^3)_p , \tag{5}$$

where $(1/r^3)_p$ is calculated between the p components of the wave function.[21] The conditions

$$a \ll g_e \mu_B H \quad \text{and} \quad |2b| \leq |\tfrac{1}{2}a|$$

being fulfilled, the ESR transitions are governed by $\Delta m_I = 0$ and $\Delta m_S = \pm 1$ in Eq. (6), where m_S and m_I are electron and nuclear magnetic quantum numbers, respectively; the magnetic field values at resonance are given by

$$H_{\parallel} = (1/g_{\parallel}\mu_B)(h\nu - m_I A_{\parallel}) \quad \text{for } \alpha = 0^\circ$$

and (6)

$$H_{\perp} = (1/g_{\perp}\mu_B)(h\nu - m_I A_{\perp}) \quad \text{for } \alpha = 90^\circ ,$$

where α is the angle between the external magnetic field $\vec{H}$ and the c axis of the crystal. This yields the values of $A_{\parallel}$ and $A_{\perp}$ to be compared with the theoretical values.

C. Wave function construction for the hole

The wave function for the hole is constructed as the linear combination

$$\phi_h(\vec{r}) = N[\alpha \phi_{2p,O^-}(\vec{r} + \vec{R}_0) + (1 - \alpha^2)^{1/2} \phi_{3p,Cl^0}(\vec{r})] , \tag{7}$$

where the coordinate system is such that the z axis is along the c axis of the crystal, the origin is at the chlorine 1 nucleus, and the chlorine 1 and oxygen ions are separated by a distance $\vec{R}_0$. In this equation ϕ_{2p,O^-} is a $2p$ orbital of the oxygen ion and ϕ_{3p,Cl^0} is a $3p$ orbital of the chlorine atom; α is an adjustable parameter which is calculated to fit the theoretical and observed hyperfine interaction parameter $A_{\parallel}^{(1)}$ of the unpaired electron with the chlorine 1 nucleus. The normalization factor N is determined by the equation

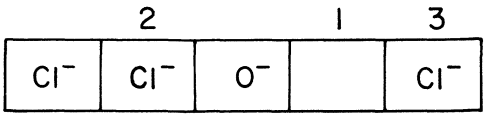

FIG. 6. Model for holelike defect II in chlorapatite corresponding to a hole h localized on an O^{2-} impurity ion, yielding an O^- ion. The O^- ion is assumed to be displaced toward the vacancy increasing the O-Cl 2 distance.

$$N=[1+2\alpha(1-\alpha^2)^{1/2}S''_{3p,2p}]^{-1/2}\ , \tag{8}$$

with

$$S''_{3p,2p}\equiv\langle\phi_{3p,\mathrm{Cl}^0}(\vec{r})\,|\,\phi_{2p,\mathrm{O}^-}(\vec{r}+\vec{R}_0)\rangle\ . \tag{9}$$

In constructing $\phi_h(\vec{r})$ [Eq. (7)], we have used the wave functions for a chlorine atom Cl^0 at site 1 and for an oxygen ion with a single negative charge O^-. This choice is meant to reflect the electron deficiency of the defect, but is somewhat arbitrary, since it is not possible to be completely consistent while employing the same orbitals for all values of α between 0 and 1. The wave function of the Cl^- ion are adopted for Cl 2 and Cl 3. The requirement that $\phi_h(\vec{r})$ be orthogonal to the neighboring ion-core orbitals is met by using the Schmidt orthogonalization procedure.

The wave function $\phi_h(\vec{r})$ is replaced by

$$\psi_h(\vec{r})=N'\Big(\phi_h(\vec{r})-\sum_i\langle\phi_h(\vec{r})\,|\,\phi_{i,\mathrm{O}^-}(\vec{r}+\vec{R}_0)\rangle\phi_{i,\mathrm{O}^-}(\vec{r}+\vec{R}_0)-\sum_j\langle\phi_h(\vec{r})\,|\,\phi_{j,\mathrm{Cl}^0}(\vec{r})\rangle\phi_{j,\mathrm{Cl}^0}(\vec{r})$$
$$-\sum_k\langle\phi_h(\vec{r})\,|\,\phi_{k,\mathrm{Cl}^-}(\vec{r}-\vec{R}_0)\rangle\phi_{k,\mathrm{Cl}^-}(\vec{r}-\vec{R}_0)-\sum_l\langle\phi_h(\vec{r})\,|\,\phi_{l,\mathrm{Cl}^-}(\vec{r}+2\vec{R}_0)\rangle\phi_{l,\mathrm{Cl}^-}(\vec{r}+2\vec{R}_0)\Big)\ , \tag{10}$$

where N' is a normalizing factor obtained from the relation

$$\langle\psi_h(\vec{r})\,|\,\psi_h(\vec{r})\rangle=1\ , \tag{11}$$

and where the indices i, j, k, and l run over the orbitals of the oxygen ion, chlorine 1, chlorine 2, and chlorine 3, respectively. In Eq. (11) the value of N', which involves products of overlap integrals, differs negligibly from unity and for present purposes we will adopt the value $N'=1$.

In Eq. (10) the wave functions for the oxygen ion, chlorine ion, and chlorine atom are derived from Clementi's tables.[22] These analytic wave functions are constructed as linear combinations of Slater orbitals. The overlap integrals are calculated using the method described by Mulliken, Rieke, Orloff, and Orloff.[23] The values of the overlap integrals are given in Table II, where

$$S_{2p,1s}\equiv\langle\phi_{2p,\mathrm{O}^-}(\vec{r}+\vec{R}_0)\,|\,\phi_{1s,\mathrm{Cl}^-}(\vec{r})\rangle\ , \tag{12}$$

$$S'_{3p,1s}\equiv\langle\phi_{3p,\mathrm{Cl}^0}(\vec{r})\,|\,\phi_{1s,\mathrm{Cl}^-}(\vec{r}-\vec{R}_0)\rangle\ , \tag{13}$$

$$S''_{3p,1s}\equiv\langle\phi_{3p,\mathrm{Cl}^0}(\vec{r})\,|\,\phi_{1s,\mathrm{O}^-}(\vec{r}+\vec{R}_0)\rangle\ , \tag{14}$$

and with $S_{2p,2s}$, $S_{2p,3s}$, $S_{2p,2p}$, $S_{2p,3p}$, $S'_{3p,2s}$, $S'_{3p,3s}$, $S'_{3p,2p}$, $S'_{3p,3p}$, $S''_{3p,2s}$, and $S''_{3p,2p}$ given by similar expressions. The wave function $\psi_h(\vec{r})$ is then used to compute $A_{\parallel}^{(1)}$ as a function of the adjustable parameter α. Using Eqs. (3)–(5), (8), and (10), one gets

$$A_{\parallel}^{(1)}=[1-0.1382\alpha(1-\alpha^2)^{1/2}]^{-1}$$
$$\times[2.06\alpha^2+(1-\alpha^2)102.2]\ \mathrm{G}\ . \tag{15}$$

Using the same set of equations, one gets

$$A_{\perp}^{(1)}=[1-0.1382\alpha(1-\alpha^2)^{1/2}]^{-1}$$
$$\times[1.09\alpha^2-(1-\alpha^2)51.6]\ \mathrm{G}\ . \tag{16}$$

The value of α is adjusted to fit the experimental value of $A_{\parallel}^{(1)}$ according to Eq. (15), which gives

$$\alpha^2=0.724\ . \tag{17}$$

This value substituted in Eq. (16) yields $A_{\perp}^{(1)}=-13.0$ G, which agrees closely with the experimental value ± 13.5 G. Furthermore, the substitutions give determinations of the signs of $A_{\parallel}^{(1)}$ and $A_{\perp}^{(1)}$. The value of α^2 given by Eq. (17) is now used to determine the hyperfine constants for the nuclei in the second and third chlorine sites for a further test of the model. These calculations employ the wave function ψ_h of Eq. (10). The results of the calculations are shown in Table III, where we compare them with the experimentally determined values. As noted above, the parameter α^2 was chosen to give the correct value of $A_{\parallel}^{(1)}$. The agreement with experiment for the remaining five hyperfine constants is excellent and lends strong support to the defect model shown in Fig. 5. In this table, predictions for the conditions $\alpha^2=1$ and $\alpha^2=0$ are also presented; the former condition corresponds to localizing the hole on the oxygen ion, while the latter corresponds to localizing the hole on Cl 1. It can be seen that neither of these choices agrees with experiment whereas the delocalized hole does.

TABLE II. Values computed for overlap integrals for a spacing of 3.382 Å between adjacent anions along the c axis. The symbols are defined in the text.

$S_{2p,1s}=0.0008054$	$S'_{3p,1s}=0.000357$
$S_{2p,2s}=0.00874$	$S'_{3p,2s}=0.0071$
$S_{2p,3s}=0.0499$	$S'_{3p,3s}=0.0538$
$S_{2p,2p}=-0.001746$	$S'_{3p,2p}=-0.0014$
$S_{2p,3p}=-0.0897$	$S'_{3p,3p}=-0.0955$
$S''_{3p,1s}=0.00145$	
$S''_{3p,2s}=0.00512$	
$S''_{3p,2p}=-0.0691$	

VI. DISCUSSION

The model for defect I shown in Fig. 5 is supported by the following arguments: (a) its ESR

TABLE III. Comparison of the values in gauss for hyperfine interactions with Cl^{35} nuclei for defect I in x-irradiated chlorapatite as determined theoretically and experimentally. The values for Cl^{37} are obtained by multiplying by the magnetic moment ratio.

	$A_{\parallel}^{(1)}$	$A_{\perp}^{(1)}$	$A_{\parallel}^{(2)}$	$A_{\perp}^{(2)}$	$A_{\parallel}^{(3)}$	$A_{\perp}^{(3)}$
Experiment	±30.3 (±0.05)	±13.5 (±0.10)	+1.55 (±0.05)	±0.80 (±0.10)	±0.94 (±0.05)	±0.40 (±0.10)
Theory						
$\alpha^2=0.724$	30.3	−13.0	1.53	0.81	0.70	0.42
$\alpha^2=1$	2.06	1.09	2.11	1.12	0	0
$\alpha^2=0$	102.2	−51.6	0	0	2.53	1.53

spectrum is axially symmetric about the pseudohexagonal c axis of the crystal; it results from a spin-$\frac{1}{2}$ holelike defect with hyperfine and superhyperfine interactions with Cl^{35} and Cl^{37} nuclei in three inequivalent chlorine sites as indicated by the computer fits shown in Fig. 3; and (b) the theoretical calculations described in Sec. V give results in agreement with the experiment. This calculation uses a single adjustable parameter to calculate six hyperfine and superhyperfine interaction constants. The agreement supports strongly the presence of an oxygen impurity ion. It is likely that this oxygen ion substitutes at a chlorine ion lattice site since the calculations were performed using an internuclear distance of 3.382 Å for the ions located on the c axis which is the normal distance between chlorine ion sites. The presence of oxygen ions in the chlorapatite structure is further supported by the fact that defect I is not observed in flux-grown chlorapatite crystals which have been grown in an HCl stmosphere. Such crystals are less likely to incorporate oxygen during the growth process than the crystals used in this study which have been grown by a flux method in air. In addition defect I is not present in hydrothermally grown crystals, which are believed to incorporate less impurity ions during the growth process.[19]

The delocalization of the hole onto an adjacent halogen, represented by $(1-\alpha^2)=0.276$, is not observed for an analogous oxygen-associated center found in fluorapatite $Ca_5(PO_4)_3F$, labeled as H II.[10] Also, in fluorapatite the value of $A_{\parallel}$ for interaction with an adjacent fluorine nucleus is much less than $A_{\parallel}^{(1)}$ in chlorapatite. These differences can be accounted for by the following reasoning. Although chlorapatite and fluorapatite have similar structures, their space groups differ; chlorapatite is monoclinic with space group $P2_1/b$ and fluorapatite is hexagonal $P6_3/m$. In fluorapatite, the fluorine ion, situated on the sixfold c axis occupies a more symmetrical position, namely the center of the calcium triangle in Fig. 2. An oxygen ion substituting for a chlorine ion in monoclinic chlorapatite experiences an asymmetry in the crystal field acting upon it which is consistent with unequal delocalization of the trapped hole on the two chlorines adjacent to the oxygen; this is not the case for the oxygen impurity ion in the hexagonal fluorapatite for which the crystal field is the same along the c axis on each side of the oxygen ion and for which the hole interacts equally with two fluorine nuclei. The asymmetry in chlorapatite arises from the fact that the chlorine ion cannot reside in the calcium triangle because of its larger ionic radius (1.80 Å). A consequence of the asymmetry is that an oxygen ion substituting for a chlorine ion in chlorapatite could, because of its smaller ionic size (1.40 Å), shift somewhat toward the plane of the calcium triangle. This shift would result in an O-Cl 1 internuclear distance shorter than the O-Cl 2 distance and would thus promote the formation of a covalent bond with resultant delocalization of the hole. The parameter α is then a measure of this covalency. The effect of this crystal-field asymmetry and the ion-size effect could explain the principal sharing of the hole between the chlorine 1 ion and the oxygen ion in chlorapatite. This is in contrast to hole localization on the oxygen ion in fluorapatite indicated by the equal hyperfine interaction of smaller magnitude with two fluorine nuclei ($A_{\parallel}=7$ G, $A_{\perp}\approx 0$).

Note that two choices had to be made somewhat arbitrarily in constructing the wave function $\psi_h(\vec{r})$ of Eq. (7). First, the overlap integrals between the oxygen and chlorine 1 orbitals were evaluated for the normal Cl-Cl distance R_0, although the present discussion suggests that a somewhat smaller distance might have been more appropriate. Second, the linear combination of Eq. (7) could have involved orbitals of a Cl^- ion, or a doubly charged oxygen ion, or both, instead of the choice actually made. Thus the extremely close agreement between experiment and theory may be somewhat fortuitous. It is expected, however, that the results of the calculation would be sufficiently insensitive to these changes that they would continue to support the model.

Another model for apparently the same center has been proposed by other authors.[17] Their model assumes the presence of a chlorine 2 ion vacancy (for the ion designation of Fig. 5) and a preferred localization of the hole on the chlorine 1 ion adjoining the oxygen ion. We rule out this possibility for two reasons. First, for this model, the values for $A_{\parallel}^{(1)}$, $A_{\parallel}^{(2)}$, and $A_{\parallel}^{(3)}$ would be 102.2, 0, and 2.53 G in strong disagreement with the experimental values. Second, this model assumes a hyperfine interaction of the hole with only two inequivalent chlorines, while our computer fit requires an interaction with chlorine in three in-

equivalent sites.

The model that we propose for defect II is shown in Fig. 6. It is derived simply from the model for defect I by assuming the presence of a chlorine-ion vacancy neighboring the oxygen ion impurity. We assume that in this model, the oxygen ion will position itself such that the vacancy replaces the chlorine 1 rather than the chlorine 2 ion. The oxygen ion relaxes towards the center of the vacancy acting as a positive attractive charge in the lattice. This explains the absence of resolved hyperfine interactions with the adjacent chlorine ions. The small calculated values of the hyperfine interaction constants shown in Table III for the hole localized on the oxygen ($\alpha^2 = 1$) adds support to this assertion. Another experimental fact supporting this model is that the concentration of defect II is increased when the chlorapatite crystals are heated *in vacuo*, a process which is known to result in an increase of the concentration of chlorine ion vacancies, due to the evolution of $CaCl_2$ from the structure.

The measured g values for defect II are similar to the g values reported for V^- holelike centers in various alkaline earth oxides. Although this type of holelike center, associated with an oxygen ion adjoining a cation vacancy, has a range of g values,[24] defect II falls within that range and has values very close to those of the V^- center in MgO.[25–27]

ACKNOWLEDGMENTS

We wish to thank Dr. E. Kostiner of the Crystal Growth Laboratory for furnishing us with untwinned chlorapatite crystals that were flux grown in air and for many helpful discussions. We also express thanks to Dr. L. Richelle for his interest and guidance in the course of this work. The computational portions of this investigation were performed at the University of Connecticut Computer Center.

---

*Supported by the U. S. Public Health Services National Institute of Dental Research Grant Nos. DE-02953 and DE-03425 and by the University of Connecticut Research Foundation.

[1]J. C. Elliott, Calc. Tiss. Res. 3, 293 (1969).
[2]G. Montel, Ann. Chim. 4, 255 (1969).
[3]L. J. Richelle and C. Onkelinx, in *Mineral Metabolism*, edited by C. Comar and F. Bronner (Academic, New York, 1969), p. 123.
[4]S. Naray-Szabo, Z. Kristallogr. 75, 387 (1930).
[5]J. S. Prener, J. Electrochem. Soc. 114, 77 (1967).
[6]P. E. Mackie, J. C. Elliott and R. A. Young, Acta Crystallogr. B 28, 1840 (1972).
[7]J. C. Elliott, Nature 230, 72 (1971).
[8]J. C. Elliott, P. E. Mackie, and R. A. Young, Science 180, 1055 (1973).
[9]M. Mengeot, M. L. Harvill, and O. R. Gilliam, J. Cryst. Growth 19, 199 (1973).
[10]B. Segall, G. W. Ludwig, H. H. Woodbury, and P. D. Johnson, Phys. Rev. 128, 76 (1962).
[11]R. K. Swank, Phys. Rev. 135, A266 (1964).
[12]W. W. Piper, L. C. Kravitz, and R. K. Swank, Phys. Rev. 138, A1802 (1965).
[13]J. S. Prener, W. W. Piper, and R. M. Chrenko, J. Phys. Chem. Solids 30, 1465 (1969).
[14]R. W. Warren, Phys. Rev. B 2, 4383 (1970).
[15]R. W. Warren, Phys. Rev. B 6, 4679 (1972).
[16]W. W. Piper and J. S. Prener, Phys. Rev. B 6, 2547 (1972).
[17]D. I. M. Knotterus, H. W. den Hartog, and W. van der Lugt, Phys. Status Solidi A 13, 505 (1972).
[18]J. S. Prener, Solid State Chem. 3, 49 (1971).
[19]A. Roufosse, M. L. Harvill, O. R. Gilliam, and E. Kostiner, J. Cryst. Growth 19, 211 (1973).
[20]*Handbook of Chemistry and Physics*, 49th ed. (The Chemical Rubber Co., Cleveland, Ohio, 1969), p. E-72.
[21]A. Abragam and B. Bleaney, *Electron Paramagnetic Resonance of Transition Ions* (Clarendon, Oxford, England, 1970), p. 173.
[22]E. Clementi, IBM J. Res. Dev. Suppl. 9, 2 (1965).
[23]R. S. Mulliken, C. A. Rieke, D. Orloff, and H. Orloff, J. Chem. Phys. 17, 1248 (1949).
[24]A. E. Hughes and B. Henderson, in *Point Defects in Solids*, edited by J. H. Crawford, Jr. and L. M. Slifkin (Plenum, New York and London, 1972), p. 381.
[25]J. E. Wertz, P. Auzins, J. H. E. Griffiths, and J. W. Orton, Discuss. Faraday Soc. 28, 136 (1959).
[26]R. C. DuVarney and A. K. Garrison, Solid State Commun. 12, 1235 (1973).
[27]W. P. Unruh, Y. Chen, and M. M. Abraham, Phys. Rev. Lett. 30, 446 (1973).